

# ELECTROCHEMICAL BEHAVIOUR OF SUPERDUPLEX UNS S 32760 (4501) STAINLESS STEEL

## COMPORTAMENTO ELETROQUÍMICO DO AÇO INOXIDÁVEL SUPERDUPLEX UNS S 32760 (4501)

Ruth Flavia Vera Villamil Jaimes<sup>1</sup>, Luis Gustavo Nunes Barbosa<sup>1</sup>,  
Monica Luisa Chaves de Andrade Alfonso<sup>2</sup>, Klester Dos Santos Sousa<sup>1</sup>,  
Silvia Maria Leite Agostinho<sup>1</sup>, Alexandre Sokolowski<sup>3</sup> & Celso Antonio Barbosa<sup>3</sup>

(1) Instituto de Química–Universidade de São Paulo (USP). São Paulo, SP, Brazil.

(2) Instituto Tecnológico e Nuclear, Unidade de Química do Estado Sólido, Sacavém, Portugal

(3) Villares Metals S. A., Sumaré, SP, Brazil.

### Abstract

Superduplex stainless steels (SDSS) have been used successfully for Oil and Gas Offshore applications. These materials present excellent resistance to localized corrosion, especially pitting resistance in sea water environments at temperatures up to 70°C, and adequate mechanical properties. SDSS UNS S 32760 (4501) presents high pitting resistance thanks to its high PREN (Pitting Resistance Equivalent Number), over 40. However the attractive properties of this SDSS may be destroyed by formation of precipitates, like Cr<sub>2</sub>N. The objective of this work is to study the effect of different microstructures in the critical pitting temperature-CPT using the solution recommended by the standard ASTM G-48-03, method E, throughout using electrochemical techniques. Two samples, A - conventional and B - improved, with different microstructures were tested to show the effect on the pitting corrosion resistance of different chemical compositions and microstructures. The results confirm that the sample B alloy presents better characteristics than the sample A. The alloys with higher PREN and less precipitation of intermetallics showed the highest CPT and higher pitting corrosion resistance (showing a pitting potential more positive). EIS studies were made also to characterize the passivating films formed on the different surfaces at the corrosion potential: the same equivalent circuit describes the electrochemical behaviour of the two samples, however the sample B presented higher polarization resistance values.

**Key-words:** Superduplex, UNS S 32760, stainless steel, passivating film, electrochemical impedance, pitting corrosion.

### Resumo

Aços inoxidáveis super duplex (AISD) têm sido utilizados com sucesso em aplicações para petróleo e gás. Estes materiais apresentam excelente resistência à corrosão localizada, principalmente em ambientes de corrosão de água do mar em temperaturas até 70°C, e propriedades mecânicas adequadas. O AISD UNS S 32760 (4501) apresenta alta resistência à corrosão, graças ao seu alto PREN (Número Equivalente de Resistência ao Pite – tradução do inglês), superior a 40. No entanto, as propriedades atraentes deste AISD podem ser destruídas pela formação de precipitados, como o Cr<sub>2</sub>N. O objetivo deste trabalho é estudar o efeito de diferentes microestruturas na CPT (Temperatura Crítica de Pite – tradução do inglês), usando a solução recomendada pela norma ASTM G-48-03 - método E, empregando técnicas eletroquímicas. Duas amostras, A - aço convencional e B - aço otimizado, com diferentes microestruturas foram testadas para mostrar o efeito sobre a resistência à corrosão de diferentes composições químicas e microestruturas. Os resultados confirmam que o aço otimizado apresenta melhores características do que o aço convencional. A liga com PREN maior e menor precipitação de intermetálicos apresentou a maior CPT. Estudos por EIS foram feitos também para caracterizar os filmes de passivação formados sobre as diferentes superfícies no potencial de corrosão. Um mesmo circuito equivalente serviu para descrever as duas amostras estudadas, no entanto, a amostra B apresentou maiores valores de resistência de polarização.

**Palavras-chave:** Superduplex, UNS S 32760, aço inoxidável, filme de passivação, impedância eletroquímica, corrosão por pite.

## Introduction

Corrosion problems are frequent and occur in various industries, such as in chemical, petroleum, marine, construction, automotive, transportation in air, rail and subway, among others. Economic losses due to corrosion can be of several forms:

- Costs of replacement parts and equipment;
- Costs of maintenance protection process;
- Shutdowns for cleaning heat exchangers or for replacement of corroded parts;
- Loss of product through corroded pipes.

The super duplex stainless steels (SDSS) offer a favorable combination of mechanical and corrosive properties, especially high resistance to stress corrosion and corrosion induced by chloride. The SDSS are steels that have higher PREN (Protection Resistance Equivalent Number) with values greater than 40.

These properties provide a huge field of application in marine and petrochemical industries, for example, subsea manifolds with associated risers, vessels, valves and heat exchangers. Many of these applications are in areas where common alloy austenitic stainless steels suffer corrosion cracking or pitting due to attack of chloride dissolved in ocean water.

The microstructure of the alloys in the SDSS austenite and ferrite phases presents in the approximate ratio of 1:1 by volume. The corrosion properties of the ferrite and austenite are dependent on the chemical composition of each phase, which in turn will result in resistance to corrosion as a whole. The main alloying elements are Cr, Mo, Ni and N where, Ni and N stabilize the austenite structure while Cr and Mo stabilize the ferrite structure.

Recent studies in the literature (Cvijovic et al., 2006 and Lo et al., 2007) have shown that the solution temperature treatment strongly affects the amount, composition and morphology of ferrite in SDSS. The authors write that the ferrite content increases as the temperature of the solution annealing treatment increases, which leads to a dilution of alpha phase forming elements such as Cr and Mo in the ferrite phase.

Some publications (Lee, 2006; Lothongkum et al., 2006; Cho ET AL., 2000) have described the structure and composition of passive films or alloy below the passive film. The addition of elements as Cr and Mo, has been recommended to increase to some extent, resistance to corrosion. Unfortunately, little is known about the effects of microstructure on the SDSS pitting corrosion. Therefore, electrochemical methods are used to evaluate the influence of chloride ion concentration and temperature on the stability of passive film on SDSS.

The objective of this work is to compare the effect of different microstructures in the critical pitting temperature-CPT and in the electrochemical behavior, using electrochemical impedance spectroscopy.

## Materials and Methods

*Working Electrode:* The samples were supplied by Villares Metals in the form of small cylinders of about 20 mm diameter and 80 mm height taken from mid radius of 152.40 mm diameter bar. The chemical composition of the conventional and the improved steels are presented in Table 1, as well as the PREN, the amounts of austenite and chromium nitride. The improved steel presents a slightly higher PREN and a higher amount of austenite. Besides this, controlled production techniques were employed to avoid the occurrence of Cr<sub>2</sub>N precipitation inside the ferrite grain boundaries (Barbosa et al., 2010).

Table 1: Chemical composition, austenite and Cr<sub>2</sub>N percentages and PREN of the conventional and improved SDSS UNS S 32760 (ASTM A 276) samples.

Steel	C	Si	Mn	Cr	Ni	Mo	N	P	S	Cu	W	Ferrite (%)	Cr <sub>2</sub> N (%)	PREN
UNS S 32760	Max 0.03	Max 1.00	Max 1.00	24.0 - 26.0	6.0 - 8.0	3.0 - 4.0	0.20 - 0.30	Max 0.030	Max 0.010	0.50 - 1.00	0.50 - 1.00	-	-	≥ 40.0
Conventional Steel	0.019	0.38	0.70	24.9	6.38	3.37	0.27	0.026	0.001	0.63	0.65	57.5	0.84	40.3
Improved Steel	0.024	0.35	0.60	25.3	6.84	3.55	0.25	0.017	< 0.001	0.54	0.63	41.3	0.01	41.02

The making of the working electrode was made by withdrawing a small barrel of crude sample and under which the soldier was a stick of brass. The set (sample + brass) was embebed in a matrix of Teflon. The working electrode was mounted and sanded with silicon carbide sand paper, whose particle sizes ranged from 120 to 2000. After grinding the sample was washed with distilled water and ethanol and then dried with hot air. After each measurement, the procedure was repeated from the sanding.

*Reference Electrode:* It was used the saturated calomel electrode ( $E_0 = 0.2444V / SHE$  as reference electrode)

*Auxiliary electrode:* It was used as auxiliary electrode a platinum plate with a relatively large area ( $20.4 \text{ cm}^2$ ) in order to promote the implementation of the current on the working electrode.

*Techniques:* Potentiodynamic polarization curves and electrochemical impedance spectroscopy.

*Equipment:* It was used the potentiostat / galvanostat microAutolab compact III, along with support softwares NOVA and GPES.

*Solution:* According to ASTM G48 - 03 standard (ASTM, 2009) -  $\text{FeCl}_3 \cdot 6\text{H}_2\text{O}$  6% + HCl 1%.

## Results and Discussion

Figure 1 shows the potentiodynamic polarization curves of conventional SDSS - sample A. The potential of current increase for each temperature corresponds to the potential where the current density exceeds  $1.10^{-4} \text{ A.cm}^{-2}$ . From 51.5°C the protective film breaks down and begins the initial occurrence of pits. For temperatures below 51.5°C the curves have practically the same behavior, showing potential of current increase above 0.85 V.

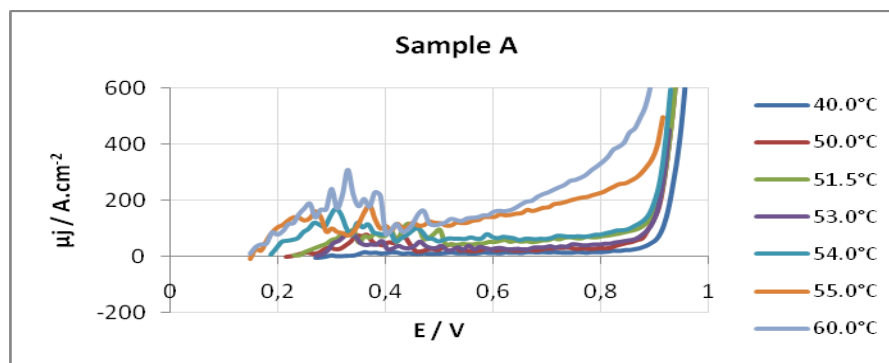


Figure 1: Potentiodynamic polarization curve of the conventional SDSS - sample A in  $\text{FeCl}_3 \cdot 6\text{H}_2\text{O}$  6% + HCl 1%..

Figure 2 shows the potentiodynamic polarization curves for the improved SDSS - sample B. This material shows a greater pitting resistance because the potential of current increase remains almost constant at around 0.84 V up to relatively high temperatures (70°C). This current increase can be attributed to oxidation of  $\text{Cr}_2\text{O}_3$  to  $\text{Cr}_2\text{O}_7^{2-}$ . Above 80°C the potential of current increase occurs at lower values due to the presence of pits.

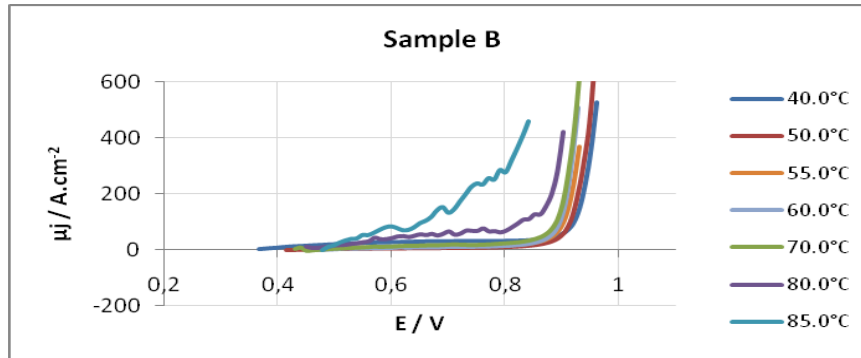


Figure 2: Potentiodynamic polarization curve of the improved SDSS - sample B in  $\text{FeCl}_3 \cdot 6\text{H}_2\text{O}$  6% + HCl 1% . .

It was possible, from polarization curves, to obtain the current density values for the two samples at 50°C: the sample A presented  $29.0 \mu\text{A} \cdot \text{cm}^{-2}$  while the sample B presented  $11.6 \mu\text{A} \cdot \text{cm}^{-2}$ . These results are an indication that sample B presents a more protective passive film.

Figures 3 and 4 show, more accurately, the pitting critical temperature for the two materials. This parameter was determined from the discontinuity of the curve “potential of current increase versus temperature”. The first section of the curve (up to 53°C in figure 3 and 80°C in figure 4) shows the potential decrease with the increase of temperature due to the decrease of the activation energy of the  $\text{Cr}_2\text{O}_3 / \text{Cr}_2\text{O}_7^{2-}$  oxidation process. In the second part of the curves (from 55°C in figure 3 and 80°C in figure 4) occurs a discontinuity in the potential of current increase; its value becomes less positive and it can be attributed to another process: the metal dissolution due to pitting corrosion.

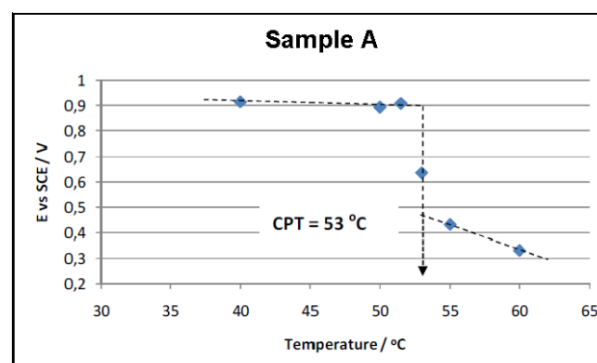


Figure 3: Critical pitting temperature evaluation for conventional SDSS - sample A

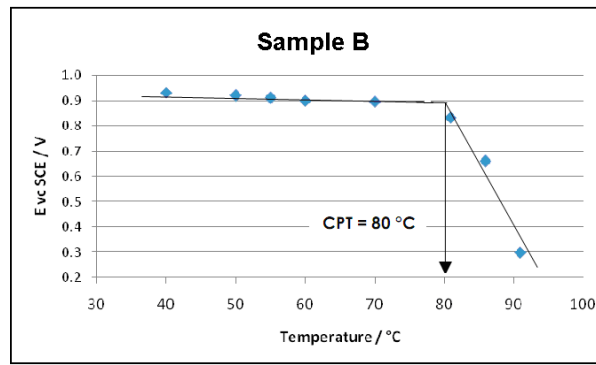
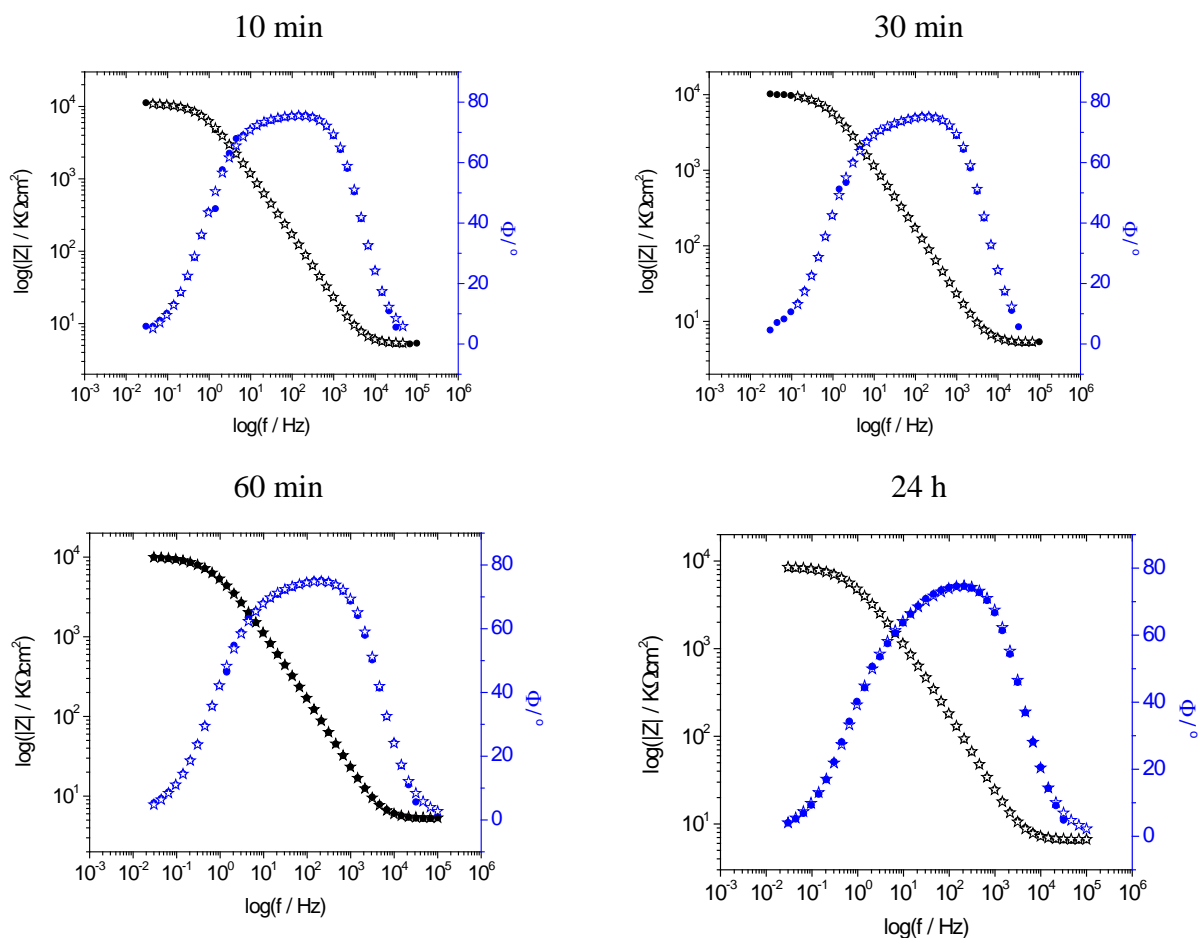


Figure 4: Critical pitting temperature evaluation for improved SDSS – sample B.

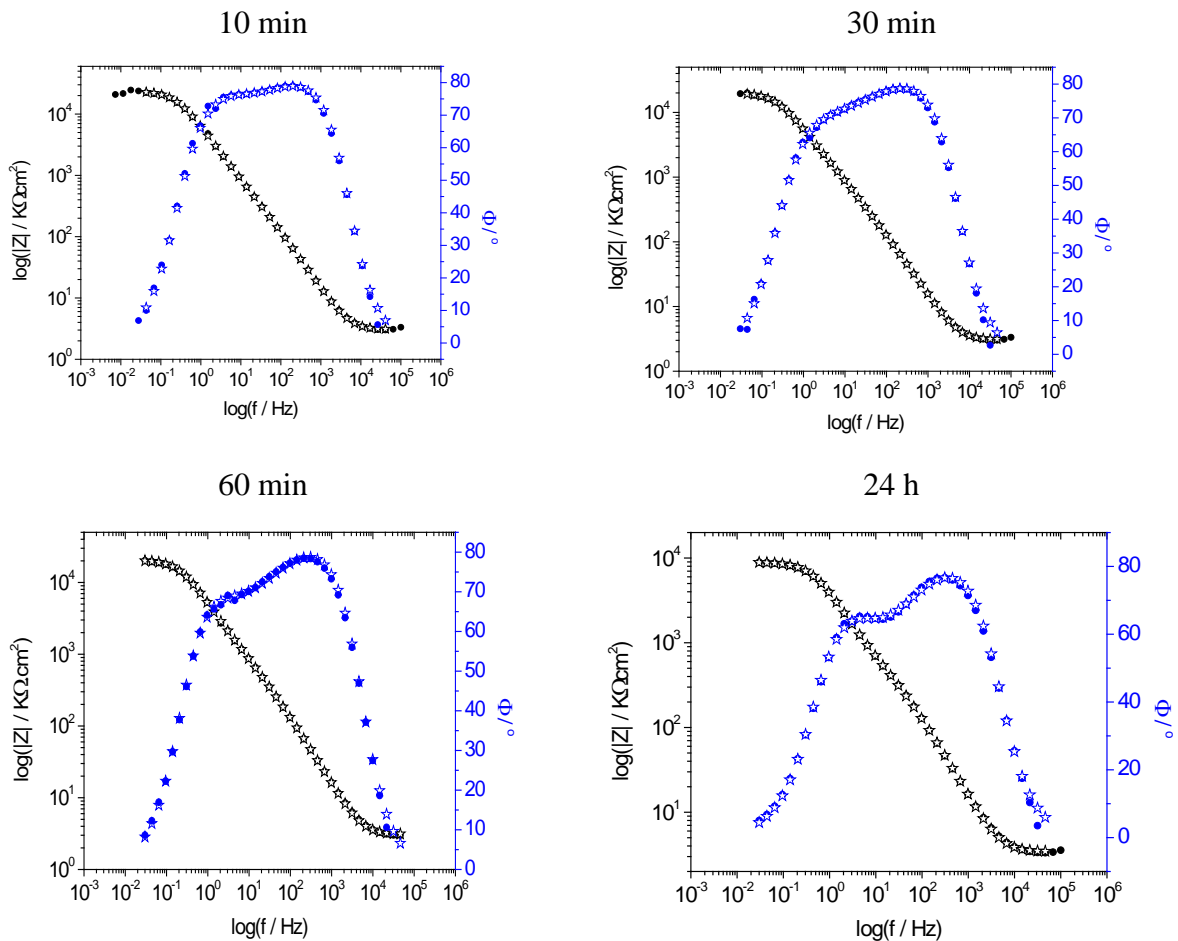
The comparison between Figures 3 and 4 shows that the improved steel - sample B - presents a pitting critical temperature 27 degrees higher than that observed for the conventional steel - sample A. The temporal evolution of the sample A and sample B (using the same solution recommended in the ASTM G48-03 standard, method E) was studied by electrochemical spectroscopy at corrosion potential at different time intervals (10 min, 30 min, 1h and 24 h) at 25°C.

Figures 5 and 6 present the Bode diagrams for the two studied steels, where the experimental results are plotted against the simulated values obtained by fitting the experimental curves to the equivalent circuit of Figure 7.



- Experimental
- ☆ Simulation

Figure 5: Impedance tests for sample A in  $\text{FeCl}_3 \cdot 6\text{H}_2\text{O}$  6% and HCl 1% at  $E_{\text{corr}}$ .



- Experimental
- ☆ Simulation

Figure 6: Impedance tests for sample B in  $\text{FeCl}_3 \cdot 6\text{H}_2\text{O}$  6% and  $\text{HCl}$  1% at  $E_{\text{corr}}$ .

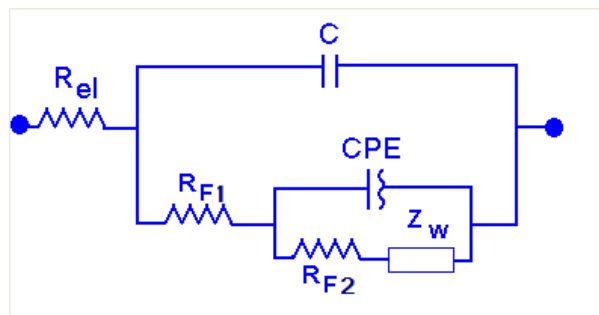


Figure 7: Electrical equivalent circuit used to fit all the experimental data at different potentials for both the studied and developed alloys.

There is a very good agreement because the curves practically coincide on the entire frequency range studied and for different immersion times. Note, that the proposed equivalent circuit, suggest that the interface must provide two films, a more compact internal, represented by  $R_{F1}$  in parallel with the capacitor  $C$  and a outer film, less compact, with  $R_{F2}$  resistance in series with the Warburg impedance characteristic of a diffusion process, and a constant phase element  $C_{PE}$ , in parallel.  $R_{EL}$  represents the resistance of the electrolyte. The values of these parameters are presented in Table 2 and 3.

Table 2: Sample A electrical parameters obtained from the simulation of experimental data to the equivalent circuit proposed. Solution: FeCl<sub>3</sub>.6H<sub>2</sub>O 6% and HCl 1%. Corrosion potential at 25°C.

t [ min ]	R <sub>el</sub> [ Ωcm <sup>2</sup> ]	R <sub>F1</sub> [ Ωcm <sup>2</sup> ]	C [ μFcm <sup>-2</sup> ]	R <sub>F2</sub> [ Ωcm <sup>2</sup> ]	Z <sub>w</sub>	CPE <sub>2</sub>		χ <sup>2</sup>
						Y <sub>0</sub> [ μFcm <sup>-2</sup> ]	n	
10	5	11000	5.99	230	2.07 x 10 <sup>-4</sup>	19.3	0.79	1.19 x 10 <sup>-3</sup>
30	5	10440	5.96	270	2.11 x 10 <sup>-4</sup>	22.2	0.77	2.11 x 10 <sup>-3</sup>
60	5	10000	6.12	128	2.03 x 10 <sup>-4</sup>	26-8	0.73	2.03 x 10 <sup>-3</sup>
1440	5	8700	5.99	2690	1.38 x 10 <sup>-4</sup>	28.9	0.79	1.38 x 10 <sup>-3</sup>

Table 3: Sample B electrical parameters obtained from the simulation of experimental data to the equivalent circuit proposed. Solution: FeCl<sub>3</sub>.6H<sub>2</sub>O 6% and HCl 1%. Corrosion potential at 25°C.

t [ min ]	R <sub>el</sub> [ Ωcm <sup>2</sup> ]	R <sub>F1</sub> [ Ωcm <sup>2</sup> ]	C [ μFcm <sup>-2</sup> ]	R <sub>F2</sub> [ Ωcm <sup>2</sup> ]	Z <sub>w</sub>	CPE <sub>2</sub>		χ <sup>2</sup>
						Y <sub>0</sub> [ μFcm <sup>-2</sup> ]	n	
10	3	23800	10.0	900	1.34 x 10 <sup>-4</sup>	17.9	0.87	2.51.10 <sup>-3</sup>
30	3	20000	9.60	6200	1.12 x 10 <sup>-4</sup>	23.6	0.93	1.77.10 <sup>-3</sup>
60	3	20600	9.38	2390	9.98 x 10 <sup>-5</sup>	23.0	0.92	2.74.10 <sup>-3</sup>
1440	3	8990	9.42	8110	9.50 x 10 <sup>-5</sup>	31.4	0.90	1.75.10 <sup>-3</sup>

Note that the values of R<sub>EL</sub> are of the order of magnitude expected for electrical resistance of the electrolyte. The very high values of R<sub>F1</sub> show that the passive film is built on the order of tens of megaohms, higher for the improved steel and decreased with time of immersion in both cases. The value of C is shown to be compatible with the capacity of the electrical double layer. Note that the value of R<sub>F2</sub> for the outer film is higher for the improved steel and grows with time, indicating the aging of the film. Z<sub>w</sub> values are higher for the conventional steel. The values of n show clearly that the film has better capacitive characteristics for the improved steel, which can also be seen by comparing the maximum of the curves of phase angle as a function of the frequency.

## Conclusions

The improved steel - sample B showed a critical temperature of pitting (CPT<sub>B</sub> = 80°C) higher than that for conventional steel - sample A (CPT<sub>A</sub> = 53°C).

Tests carried out by electrochemical impedance at the corrosion potential showed very good agreement with the simulation results using equivalent circuits. The simulation showed that the same equivalent circuit model describes the electrochemical behavior of the two samples. According to the proposed equivalent circuit, there is a compact inner film and other outer film that is porous.

The sample B had its surface covered with a passivating film with the same characteristics present in the sample A at all immersion time studied, however the resistances of the films are higher for sample B then those one observed for sample A.

## **Bibliography**

AMERICAN SOCIETY FOR TESTING AND MATERIALS (ASTM). G 48-03: Standard test methods for pitting and crevice corrosion resistance of stainless steels and related alloys by use of ferric chloride solution. In: **Annual Book of ASTM Standards**, Philadelphia: 2009.

Barbosa, C. A. and Sokolowski, A. Development of UNS S 32760 superduplex stainless steel produced in large diameters rolled bars. **CD-ROM Proceeding**, 10<sup>th</sup> Brazilian Stainless Steel Conference, Rio de Janeiro, 2010.

Cho, E-A.; Kim, C-K.; Kim, J-S.; Kwon, H-S. Quantitative analysis of repassivation kinetics of ferritic stainless steels based on the high field ion conduction model. **Electrochimica Acta**; Vol 45, Issue 12, pages 1933–1942. February 2000

Corrosion of Metals and Alloys - Corrosivity of atmospheres - Determination of corrosion rate of standard specimens for the evaluation of corrosivity, **ISO 9226 standard**, 1992.

Cvijovic, Z. and Radenkovic, G. Microstructure and pitting corrosion resistance of annealed duplex stainless steel. **Corrosion Science**, Vol 48, Issue 12, pages 3887–3906, December 2006.

Lee, J. Effects of alloying elements, Cr, Mo and N on repassivation characteristics of stainless steels using the abrading electrode technique. **Materials Chemistry Physics**, Vol 99, Issues 2-3, pages 224–234, October 2006;

Lo, K. H.; Lai, J. K. L.; Shek, C. H.; Li, D. J. Effects of pre-treatment on the ac magnetic susceptibility and ageing behavior of duplex stainless steels. **Materials Science and Engineering: A**; Vol 452–453, pages 78–86, April 2007.

Lothongkum, G.; Wongpanya, P.; Morito, S.; Furuhashi, T.; Maki, T. Effect of nitrogen on corrosion behavior of 28Cr–7Ni duplex and microduplex stainless steels in air-saturated 3.5 wt% NaCl solution. **Corrosion Science**; Vol 48: pages 137–153. February 2005.

## **Author's E-mail's:**

Ruth Flavia Vera Villamil Jaimes: e-mail: rfvillam@iq.usp.br

Luis Gustavo Nunes Barbosa: e-mail: luis.barbosa@poli.usp.br

Monica Luisa Chaves de Andrade Alfonso: e-mail: mochaves@sapo.pt

Klester Dos Santos Sousa: e-mail: klester@iq.usp.br

Silvia Maria Leite Agostinho: e-mail: smlagost@iq.usp.br

Alexandre Sokolowski: e-mail: alexandre.sokolowski@villaresmetals.com.br

Celso Antonio Barbosa: e-mail: celso.barbosa@villaresmetals.com.br